

DESIGNING CAPTURE TRAJECTORIES TO UNSTABLE PERIODIC ORBITS AROUND EUROPA *

Ryan P. Russell[†] and Try Lam[‡]

The hostile environment of third body perturbations restricts a mission designer's ability to find well-behaved reproducible capture trajectories when dealing with limited control authority as is typical with low-thrust missions. The approach outlined in this paper confronts this shortcoming by utilizing dynamical systems theory and an extensive pre-existing database of Restricted Three Body Problem (RTBP) periodic orbits. The stable manifolds of unstable periodic orbits are utilized to attract a spacecraft towards Europa. By selecting an appropriate periodic orbit, a mission designer can control important characteristics of the captured state including stability, minimum altitudes, characteristic inclinations, and characteristic radii among others. Several free parameters are optimized in the non-trivial mapping from the RTBP to a more realistic model. Although the ephemeris capture orbit is ballistic by design, low-thrust is used to target the state that leads to the capture orbit, control the spacecraft after arriving on the unstable quasi-periodic orbit, and begin the spiral down towards the science orbit. The approach allows a mission designer to directly target fuel efficient captures at Europa in an ephemeris model. Furthermore, it provides structure and controllability to the design of capture trajectories that reside in a chaotic environment.

INTRODUCTION

Typical science orbits at Europa require close proximity to the surface and high inclinations to provide global coverage for mapping purposes. Capturing directly to these orbits using low-thrust is impossible because of the forbidden regions associated with the dynamics of the RTBP. A capture trajectory with limited control authority is thus restricted to higher altitude orbit insertions. Furthermore, a host of recent studies have re-emphasized that the high-inclination mapping orbits are unstable [1,2,3,4,5], and increasingly so at the higher altitudes where low-thrust captures are feasible.

Distant Retrograde Orbits (DROs) exist in the ephemeris model at Europa well beyond 50,000 km and are extremely stable when the out of plane motion is small [4]. As a result, a typical and rather straightforward approach for designing a capture orbit at Europa follows the path of inserting into a near-planar DRO and then systematically changing the characteristic radius and inclination until a science orbit is achieved [6,7,8]. Although this approach is inherently less risky, it can be costly both in time and fuel [8]. Thus, we proceed by outlining a capture technique that provides mission designers the improved ability to target a variety of close highly-inclined capture orbits with little thrusting capabilities even in the highly unstable regions of the design space.

Recent applications of dynamical systems theory to the multi-body astrodynamics problem have led to a new paradigm of trajectory design [9,10,11,12,13,14,15,16]. From this perspective, trajectories exploit natural unstable dynamics to efficiently navigate through chaotic regions in phase space [17]. The perturbing effects of a secondary gravitating body in the vicinity of a spacecraft and a primary body can be utilized to capture or escape the primary using little or no fuel. These attracting or repelling trajectories comprise a stable or unstable manifold of orbits, respectively. The set of these manifolds mapped for the many attracting

* Presented as Paper AAS 06-189 for the 2006 AAS/AIAA Space Flight Mechanics Meeting in Tampa, Florida

[†] Engineer, Jet Propulsion Laboratory, 4800 Oak Grove Drive, M/S 301-140L, Pasadena, California 91109.

Email: Ryan.Russell@jpl.nasa.gov. Member AIAA, AAS

[‡] Engineer, Jet Propulsion Laboratory, 4800 Oak Grove Drive, M/S 301-125L, Pasadena, California 91109.

Email: Try.Lam@jpl.nasa.gov. Member AIAA, AAS

bodies in the Solar System comprise what is commonly referred to as the *Interplanetary Superhighway* [18]. The paths of these manifolds trace chaotically through the solar system, and intersections of two manifolds provide mechanisms to ballistically connect two seemingly isolated regions [19]. These concepts have been successfully demonstrated in flight missions such as ISEE-3 (International Sun-Earth Explorer-3), ACE (Advanced Composition Explorer), SOHO (Solar and Heliospheric Observatory), and Genesis among others [20,21,22,23,24].

Although the manifolds associated with the halo family have been the focus of the most recent applications in this area, there are scores of other families of periodic orbits and associated invariant manifolds that have received much less attention. In this paper, we tap into this potential by using an extensive database of previously computed periodic orbits in the vicinity of Europa as attracting mechanisms for capture [25]. The structure of the manifolds [26] of these more complicated orbits is much more erratic in general than the manifolds that emanate from the simple Halo orbits and constitute the bulk of the *Interplanetary Superhighway* (or for the case of Europa the *Intermoon Superhighway*). Perhaps the individual trajectories that make up the complicated manifolds are more akin to one-lane county roads than a superhighway; nonetheless, they are capable of providing efficient ballistic captures to orbits with specific selected characteristics. While the halo orbits manifolds can certainly be used to initiate capture orbits at Europa [8], powered maneuvers (albeit small) are necessary to complete the capture. Furthermore, the unstable nature of the orbits makes it difficult for a mission designer to control the final characteristics of the capture state. By utilizing the manifolds of the capture orbit directly, the natural dynamics are exploited to allow the spacecraft to coast to its capture state rather than taking the traditional path of fighting the dynamics with thrusting. Note that thrusting is reserved for changing orbital energy and controlling the spacecraft once it arrives on the quasi-periodic ephemeris orbit.

The first section of this paper gives an overview of the relevant dynamics and models. The next section outlines the algorithm to systematically design a capture orbit at Europa using limited control authority. The initial conditions of several promising attracting periodic orbits are presented along with the characteristics of the associated stable manifolds. Although all of the attracting orbits are unstable by design, some of the examples are selected because of their proximity to a recently observed class of direct near-circular periodic orbits that are stable at surprisingly high inclinations [25,27]. The subtleties associated with mapping these simple model manifolds into a realistic model are explored and a variety of parameters are introduced and optimized to ensure continuous ballistic captures in the full ephemeris model. Finally, we walk through an example application of a low-thrust transfer from Ganymede to a captured state at Europa, and conclusions are drawn in the final section.

The capture technique is efficient in terms of spacecraft fuel because it allows for the design of close, highly-inclined captures thus reducing the need for expensive plane changes to achieve near polar science orbits. Furthermore, the technique reduces design time because it is systematic and provides controllability over the qualities of the capture state despite the generally chaotic dynamic environment.

DYNAMICAL MODELS AND BACKGROUND

Relevant background and model information is presented for periodic orbits and manifolds in the context of both the RTBP and a realistic ephemeris model.

RTBP Equations of Motion

The equations of motion for a non-thrusting spacecraft in the Restricted Three Body Problem are presented in Equation (1) in the standard rotating frame that assumes Europa and Jupiter orbit their common center of mass with a constant separation of 1 length unit (LU) and an orbital rate of 1 radian per time unit (TU). The coordinate frame is centered at Europa, the x axis points along the Jupiter-Europa line, and the z axis points toward the system angular momentum. The spacecraft distances to Europa and Jupiter are denoted as r_E and r_J respectively. The gravitational parameters for Europa and Jupiter are Gm_E and Gm_J respectively.

$$\dot{\mathbf{X}} = \mathbf{f}(\mathbf{X}) \quad (1)$$

where,

$$\mathbf{X} = [x \ y \ z \ u \ v \ w]^T$$

$$\mathbf{f} = \begin{bmatrix} u \\ v \\ w \\ 2v + (x+1-\mu) + \kappa(x+1) + \mu/r_E^3 \\ -2u + y + \kappa y \\ \kappa z \end{bmatrix}$$

$$\kappa = -(1-\mu)/r_J^3 - \mu/r_E^3$$

$$\mu = Gm_E / (Gm_J + Gm_E)$$

$$r_J = \sqrt{(x+1)^2 + y^2 + z^2}$$

$$r_E = \sqrt{x^2 + y^2 + z^2}$$

$$J = (x+1-\mu)^2 + y^2 + 2(1-\mu)/r_J + 2\mu/r_E - u^2 - v^2 - w^2 \quad (2)$$

The Jacobi constant is an integral of motion and exists in the form given in Equation (2). Therefore, in the RTBP the Jacobi constant or energy of a spacecraft can only be changed via thrusting. For the unthrust case at a fixed value of J and velocity of zero, Equation (2) can be solved for a surface in position space that represents the boundary between valid and forbidden regions for the spacecraft. This is known as the zero-velocity surface and is illustrated in Figure 1. The neck seen in part (d) is known as Hill's neck. When its radius shrinks to zero, ballistic transfers to and from the vicinity of Europa are no longer possible. Thus an upper bound is established for the Jacobi energy for potential transfer orbits ($\sim 3.0036 \text{ LU}^2/\text{TU}^2$). This upper bound on Jacobi energy maps to a lower bound on capture orbit altitudes. For inclined near-circular orbits, this equates to approximately a 5,000 km orbit around Europa [27].

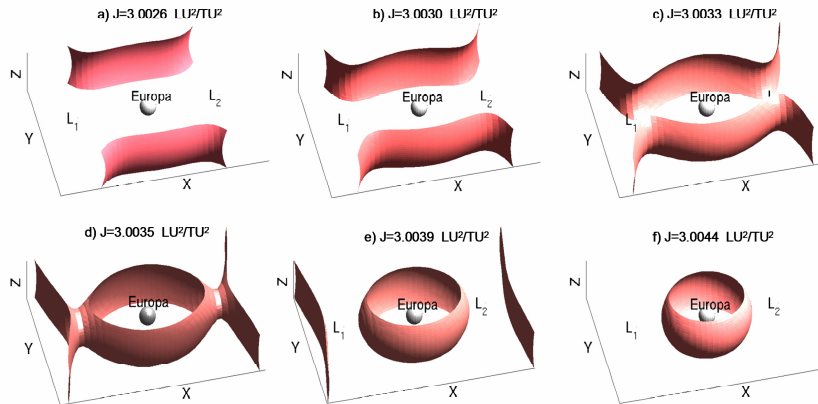


Figure 1: Zero velocity surfaces for Europa. The surfaces are sliced in order for Europa to be visible. The valid regions are near Europa. Note the closing of the neck from (d) to (e).

For the thrusting case, the spacecraft mass becomes a state variable and is governed by Equation (4). The thrust acceleration term in Equation (4) must be included in the velocity derivative terms given in the last three entries of \mathbf{f} in Equation (1). Note that Γ is the rocket thrust magnitude and the product $g_0 I_{sp}$ is the rocket exhaust velocity where I_{sp} is given in units of time and g_0 is the acceleration of gravity at the surface of Earth.

$$dm/dt = -\Gamma / (g_0 Isp) \quad (3)$$

$$\Gamma = \begin{bmatrix} \Gamma_x & \Gamma_y & \Gamma_z \end{bmatrix}^T / m \quad (4)$$

Table 1: Jupiter Europa RTBP parameters

Parameter	Symbol	Value	Comment
Europa gravitational parameter	Gm_E	3202.72 km ³ /sec ²	Reference [28]
Jupiter gravitational parameter	Gm_J	1.2668654 × 10 ⁸ km ³ /sec ²	Reference [28]
Jupiter-Europa distance (length unit)	LU	670,900 km	Reference [28]
Europa mean radius	-	1560.7 km	Reference [28]
Mass ratio	μ	2.52800260797625 × 10 ⁻⁵	Calculated from Equation (1)
Time Unit	TU	48822.0443306681 s	Calculated time for Europa to traverse one radian. Based on circular velocity at the Europa mean radius
Velocity Unit	VU	13.7417432882581 km/s	Length unit divided by time unit

Attracting and Repelling Periodic Orbits

We proceed with a brief discussion on the stability of periodic orbits and an explanation why unstable periodic orbits share attracting and repelling qualities. A small perturbation $\delta\mathbf{X}(t_0)$ to the initial conditions of a ballistic reference trajectory \mathbf{X}^* is linearly mapped forward to a perturbation at a later time with the well known state transition matrix, Φ .

$$\delta\mathbf{X}(t) = \Phi(t, t_0)\delta\mathbf{X}(t_0) \quad (5)$$

The state transition matrix is obtained by integrating the variational equations given in Equation (6). For a detailed derivation, see for example References [25] and [29].

$$\dot{\Phi}(t, t_0) = (\partial\mathbf{f}/\partial\mathbf{X})|_* \Phi(t, t_0) \quad (6)$$

$$\Phi(t_0, t_0) = \mathbf{I}$$

For the unthrust RTBP, the partial derivative required in Equation (6) is given in Equation (7).

$$(\partial\mathbf{f}/\partial\mathbf{X}) = \begin{bmatrix} \mathbf{0}_{3 \times 3} & \mathbf{I}_{3 \times 3} \\ \mathbf{G}_{3 \times 3} & \mathbf{H}_{3 \times 3} \end{bmatrix} \quad \mathbf{H} = \begin{bmatrix} 0 & 2 & 0 \\ -2 & 0 & 0 \\ 0 & 0 & 0 \end{bmatrix} \quad (7)$$

$$G_{1,1} = (1 - \mu) \left[2(x+1)^2 - y^2 - z^2 \right] / r_J^5 + \mu (2x^2 - y^2 - z^2) / r_E^5 + 1$$

$$G_{2,2} = (1 - \mu) \left[2y^2 - (x+1)^2 - z^2 \right] / r_J^5 + \mu (2y^2 - x^2 - z^2) / r_E^5 + 1$$

$$G_{3,3} = (1 - \mu) \left[2z^2 - (x+1)^2 - y^2 \right] / r_J^5 + \mu (2z^2 - x^2 - y^2) / r_E^5 + 1$$

$$G_{1,2} = G_{2,1} = 3(1 - \mu)(x+1)y / r_J^5 + 3\mu xy / r_E^5$$

$$G_{1,3} = G_{3,1} = 3(1 - \mu)(x+1)z / r_J^5 + 3\mu xz / r_E^5$$

$$G_{2,3} = G_{3,2} = 3(1 - \mu)yz / r_J^5 + 3\mu yz / r_E^5$$

The state transition matrix evaluated after a full period, $t=T$, of a periodic orbit is commonly called the Monodromy matrix [30]. It maps an initial state perturbation vector across one full period. The norm of this matrix is defined by Equation (8) [31].

$$\|\Phi(T, t_0)\| = \text{lub}_{\|\delta\mathbf{X}(t_0)\|=1} \|\Phi(T, t_0)\delta\mathbf{X}(t_0)\| \quad (8)$$

If the norm is greater than 1, perturbations will tend to grow and trajectories will repel the reference periodic orbit. Likewise, if the norm is less than 1, perturbations will tend to damp out and trajectories will be attracted to the reference orbit. The norm of a matrix is associated with the direction of greatest amplification or the most unstable direction. However, the basis of a six dimensional space consists of six directions, where each direction can be stable, unstable, or neutral. The generalized eigen-vectors provide a convenient basis to evaluate all six directions. An eigenvalue, λ (real or complex), of the Monodromy matrix is a scalar proportionality factor that satisfies the relation:

$$\Phi(T, t_0)\xi = \lambda \xi \quad (9)$$

Thus for an eigenvalue with a magnitude greater than unity, perturbations in the eigen-direction, ξ , will grow after one period, and the orbit is unstable in this direction. It is well known that the eigenvalues of the Monodromy matrix occur in reciprocal pairs [32]. Additionally, for the RTBP, one of the eigenvalues will be unity due to the existence of the Jacobi integral [30, 32]. The eigenvalues of the Monodromy matrix for the three-dimensional RTBP will therefore have the form $\{\lambda_1, 1/\lambda_1, \lambda_2, 1/\lambda_2, 1, 1\}$. Thus, if a periodic orbit has an eigen-direction that leads to an expansion, then there is also an accompanying eigen-direction that leads to a contraction. Therefore, all eigenvalues must have a magnitude of 1 for stability in all six directions, and lastly, all unstable periodic orbits have directions that lead to both attracting and repelling trajectories.

A stable or unstable manifold is comprised of trajectories that approach or leave in forward time a periodic orbit in the direction of a stable or unstable eigen-direction respectively. From Equation (9), it is clear that the degree of stability or instability is reflected in the magnitude of the associated eigenvalue, where values less or greater than unity are increasing stable or unstable respectively. While the unstable manifolds are equally useful for general mission design, the remainder of this study focuses on the stable manifolds and their application to capture orbits.

Ephemeris Model Considerations

The RTBP model is convenient because it enables fast numerical analysis and accurately represents to first order the motion of many real three-body systems. In addition, its autonomous Hamiltonian nature leads to many niceties including the abundant existence of periodic orbits, the availability of an integral of motion, and a simplified Monodromy matrix. However, in general, the difference between the RTBP and a more realistic model is non trivial; and surprisingly, a small percentage of astrodynamics applications to dynamical systems theory include this final step of finding the trajectories in a full ephemeris model. In this paper, we pay careful attention to the ephemeris model by optimizing over several mapping parameters such that the final capture orbits are ballistic in the realistic model.

The typical approach for continuing a RTBP solution to the ephemeris model involves breaking the trajectory into several legs and mapping the initial conditions for each leg to the ephemeris model. Next, a multiple shooting method is implemented using a differential corrector and/or optimizer to drive the ephemeris model legs towards continuity[16]. This process is increasingly difficult for long and complicated trajectories and there is no guarantee that a completely ballistic ephemeris trajectory exists, especially in cases where the physical models are not as well represented by the assumptions of the RTBP. This common approach preserves the trajectory shape even for highly unstable orbits.

We take an alternative approach that does not necessarily preserve the trajectory shape, but removes the necessity for multiple legs and ensures continuity, i.e. a ballistic capture. Note that a captured state in this context is a loosely defined term meaning that the spacecraft is on an ephemeris version of a ballistic attracting trajectory associated with the stable manifold of the RTBP periodic orbit. Depending on the stability characteristics of the attracting periodic orbit, the spacecraft, if left uncontrolled, will typically complete on the order of a few revolutions around Europa before falling off the periodic orbit on one of its unstable manifolds. It is possible to design an active control scheme for orbit maintenance to keep the spacecraft in the vicinity of the reference orbit. The active control strategy is appropriate if the attracting periodic orbit is part of a mapping orbit or indefinite parking orbit that is explicit to the mission design.

However, in the case of the present application the attracting periodic orbit is employed only as a mechanism to achieve some intermediate captured state near Europa with important but loosely defined qualities, such as characteristic radii, inclination, and minimum and maximum altitudes. It is not critical that the final ephemeris capture trajectory be exactly analogous to its cousin orbit in the RTBP. Rather, it is only important that the qualities are similar and that the ephemeris attracting trajectory is ‘well-behaved’ meaning it is somewhat robust to small perturbations and it does indeed ballistically follow a stable manifold towards a captured (albeit unstable) state at Europa.

The proposed mapping from a normalized RTBP state to a dimensioned state in the true ephemeris consists of two steps: First, un-normalizing the state in the RTBP and second, doing the appropriate rotations to a non-rotating inertial state. Typically, the normalized RTBP position and velocity vectors are dimensioned using the length unit (LU) and velocity unit (VU) given in Table 1. We propose a slight variation that provides a degree of freedom in the mapping. The distance from Jupiter to Europa in reality varies on the order of a few percent of its nominal value. Among many of the non-autonomous forcing functions that drive a real ephemeris, this pulsating feature of the radius introduced by a non circular orbit is the largest perturbation to the assumptions of the RTBP. The length unit from Table 1 represents the average value of this pulsating radius. However to account for the few percent in variation, we introduce a k scaling factor in Equation (10) that provides new length units, time units, and velocity units for a RTBP system with a slightly modified characteristic length. The time and velocity units do not scale linearly because they are derived from the length unit. By varying k from 0.97 to 1.03, the resulting dimensioned states are scaled appropriately for positions and velocities. The variation is well within the noise of the ephemeris perturbations, and this scaling factor provides a convenient one dimensional degree of freedom that can be very useful in constrained problems such as the present case of searching for ballistic ephemeris capture trajectories. The k scaling technique has proven useful in References [27] and [33].

$$\text{LU}^* = k (\text{LU}) \quad \text{TU}^* = \sqrt{k^3} (\text{TU}) \quad \text{VU}^* = \sqrt{1/k} (\text{VU}) \quad (10)$$

Once Equation (10) is used to un-normalize a state for a given k value, the inertial directions of the instantaneous Jupiter-Europa line and the system angular momentum are used to define a coordinate rotation to the true ephemeris. Equations (11) and (12) provide the mappings for position and velocity vectors. The superscript indicates an un-normalized vector in the RTBP and the subscripts E and J refer to Europa and Jupiter respectively. It is assumed that the ephemeris velocity of Europa with respect to Jupiter is the time derivative of the ephemeris position (although the position and velocities may in fact be estimated independently leading to a minor violation of this principle). We also assume that the angular momentum vector, \mathbf{h}_{EJ} , is a constant although this is not true in general.

$$\mathbf{r} = \mathbf{R}\mathbf{r}^{\text{RTBP}} \quad (11)$$

$$\mathbf{v} = \dot{\mathbf{R}}\mathbf{r}^{\text{RTBP}} + \mathbf{R}\mathbf{v}^{\text{RTBP}}$$

where,

$$\begin{aligned} \mathbf{R} &= [\hat{\mathbf{x}} \mid \hat{\mathbf{y}} \mid \hat{\mathbf{z}}] & \dot{\mathbf{R}} &= [\dot{\hat{\mathbf{x}}} \mid \dot{\hat{\mathbf{y}}} \mid \dot{\hat{\mathbf{z}}}] & (12) \\ \hat{\mathbf{x}} &\equiv \frac{\mathbf{r}_{EJ}}{r_{EJ}} = \frac{\mathbf{r}_E - \mathbf{r}_J}{|\mathbf{r}_E - \mathbf{r}_J|} & \dot{\hat{\mathbf{x}}} &= \frac{\mathbf{v}_{EJ}}{r_{EJ}} - \frac{\mathbf{r}_{EJ}\dot{r}_{EJ}}{r_{EJ}^2} \\ \hat{\mathbf{z}} &\equiv \frac{\mathbf{h}_{EJ}}{h_{EJ}} = \frac{(\mathbf{r}_E - \mathbf{r}_J) \times (\mathbf{v}_E - \mathbf{v}_J)}{|(\mathbf{r}_E - \mathbf{r}_J) \times (\mathbf{v}_E - \mathbf{v}_J)|} & \dot{\hat{\mathbf{z}}} &\cong \mathbf{0} \\ \hat{\mathbf{y}} &\equiv \hat{\mathbf{z}} \times \hat{\mathbf{x}} & \dot{\hat{\mathbf{y}}} &= \dot{\hat{\mathbf{z}}} \times \hat{\mathbf{x}} \\ & & \dot{r}_{EJ} &= \mathbf{r}_{EJ}^T \mathbf{v}_{EJ} / r_{EJ} \end{aligned}$$

The ephemeris positions, velocities, and orientations of the planets and moons are provided by the DE405, jup230, and pck00008.tpc estimated solutions and are publicly available[†] from the Jet Propulsion Laboratory[34]. The body poles and prime meridians are based on the most recent data from the IAU/IAG

[†] URL: <http://naif.jpl.nasa.gov/naif/spiceconcept.html> [cited 8 Oct 2005].

URL: ftp://naif.jpl.nasa.gov/pub/naif/generic_kernels/spk/satellites/jup100.bsp [cited 8 Oct 2005].

URL: ftp://naif.jpl.nasa.gov/pub/naif/generic_kernels/spk/planets/de405_2000-2050.bsp [cited 8 Oct 2005].

URL: ftp://naif.jpl.nasa.gov/pub/naif/generic_kernels/pck/pck00008.tpc [cited 8 Oct 2005].

Working Group on Cartographic Coordinates and Rotational Elements of the Planets and Satellites [35]. Table 3 gives the gravitational parameters for all of the active bodies for the ephemeris model in this study. Table 2 provides the gravity fields terms for Jupiter and Europa based on the standard spherical harmonic expression of the potential [36]. Although this study focuses primarily on finding the initial conditions that lead to ballistic capture states, the final targeting and optimization is performed with Mystic, a high-fidelity low-thrust optimization tool under development at the Jet Propulsion Laboratory [37].

Table 2: Ephemeris model active oblateness parameters

<i>Body</i>	<i>Term</i>	<i>Normalized^a</i>	<i>Value^b</i>
Jupiter	Gm (km ³ /sec ²)	-	1.26686537.857796E+08
Jupiter	Radius (km)	-	7.149200000000000E+04
Jupiter	J2	no	1.4696429000697847E-02
Jupiter	J3	no	-6.436411055625769E-07
Jupiter	J4	no	-5.871402915754995E-04
Jupiter	J6	no	3.425025517100406E-05
Jupiter	C22	no	6.529032795399768E-09
Jupiter	S22	no	-1.249373515670649E-08
Europa	Gm (km ³ /sec ²)	-	3.200999806720590E+03
Europa	Radius (km)	-	1.562700000000000E+03
Europa	J2	yes	1.921114544207288E-04
Europa	J3	yes	-7.039660444099072E-05
Europa	C21	yes	1.151627764866707E-07
Europa	C22	yes	2.000074134884866E-04
Europa	C31	yes	-3.196687887816629E-05
Europa	C32	yes	-1.130987507887575E-05
Europa	C33	yes	-3.735793516136421E-06
Europa	S21	yes	1.151627764866707E-07
Europa	S22	yes	-4.617239150205956E-06
Europa	S31	yes	-2.362087547330383E-05
Europa	S32	yes	-3.906571822592933E-06
Europa	S33	yes	6.497673093152606E-06

^b See Reference [36] for the standard normalization for spherical harmonic terms
^a Parameters come from Mystic default files. Note, the Europa Gm, J2, and C22 are based on Galileo data, the other gravity terms are simply representative of an expected field.

Table 3: Ephemeris model active bodies and gravitational parameters

<i>Body</i>	<i>Value (km³/sec²)</i>	<i>Ephemeris</i>
Sun	132712440017.987	DE405
Mercury	22032.0804864179	DE405
Venus	324858.59882646	DE405
Earth	398600.432896939	DE405
Moon	4902.80058214776	DE405
Mars	42828.3142580671	DE405
Jupiter	See oblate Jupiter parameters from Table 2	jup100
Saturn	37940626.0611373	DE405
Uranus	5794549.00707187	DE405
Neptune	6836534.06387926	DE405
Io	5961.00007464437	jup100
Europa	See oblate Europa parameters from Table 2	jup100
Ganymede	9886.99742842995	jup100
Callisto	7180.99840324153	jup100

BALLISTIC CAPTURE ALGORITHM

In this section, an algorithm is described to obtain the initial conditions that lead to a ballistic capture orbit with user defined characteristics. It is assumed that we begin with a trajectory that approaches Europa with appropriate energy and positioning such that a ballistic capture is feasible. Obtaining such a trajectory is non-trivial, but attainable via successive resonant flybys of Europa and limited control authority typical to low-thrust or fuel-limited missions [37].

1. Select a target RTBP Periodic Orbit

As a result of the chaotic nature of the RTBP, a trajectory that approaches Europa in the neighborhood of a ballistic capture orbit can be altered dramatically with small changes in the upstream state. This sensitivity can be exploited to capture directly to orbits with dramatically different characteristics for very small fuel expenditures. We achieve this by carefully selecting attracting unstable periodic orbits that have qualities consistent with a desired capture state. For the case of the Jupiter-Europa system, Reference [25] archives over 616,000 periodic orbits with a variety of defining characteristics. Most of the solutions are unstable and thus have stable manifolds that are candidates for capture orbit applications. The defining qualities associated with each solution include the Jacobi constant, period, characteristic inclination, characteristic radius, minimum altitude, maximum altitude, ratio of the minimum to maximum altitude, and number of *xz* plane crossings among others. A database of the solutions is established such that a mission designer can filter all of the characteristics to find a periodic orbit or a range of periodic orbits that are suitable candidates for attracting mechanisms to Europa.*

* For an electronic copy of the Europa Periodic Orbit Database, send an email request to Ryan.Russell@jpl.nasa.gov. Otherwise, all differential correctors and methods to recreate such a database are described in Reference [25].

For capture applications with mapping orbit destinations, the most appealing periodic orbits are those that are close to Europa, have large characteristic inclinations, and have a minimum to maximum altitude ratio near unity. Other families of orbits such as the Halo, Lisajous, Lyapunov, or combination families have potential application for capture and other trajectory design; however, in this study we restrict our focus to periodic orbits that resemble high-altitude mapping orbits in order to minimize the complexity and cost of spiraling down from the ballistic capture state to the final low-altitude highly inclined, near circular science orbit. Figure 2 illustrates a sampling of unstable highly-inclined periodic orbits that continuously orbit Europa at Energy levels that are feasible for ballistic capture. Table 4 gives the initial conditions and characteristics for each orbit. The solutions are generated using the mass ratio given in Table 1. The direct orbits in Figure 2(c-f) are specifically chosen due to their proximity to a class of highly-inclined stable periodic orbits recently identified in References [25] and [27]. Despite the instability of the orbits in Figure 2(c-f), it is hoped that the proximity to stable regions will reduce the amount of control authority necessary to fight the perturbations as the spacecraft spirals down to a science orbit.

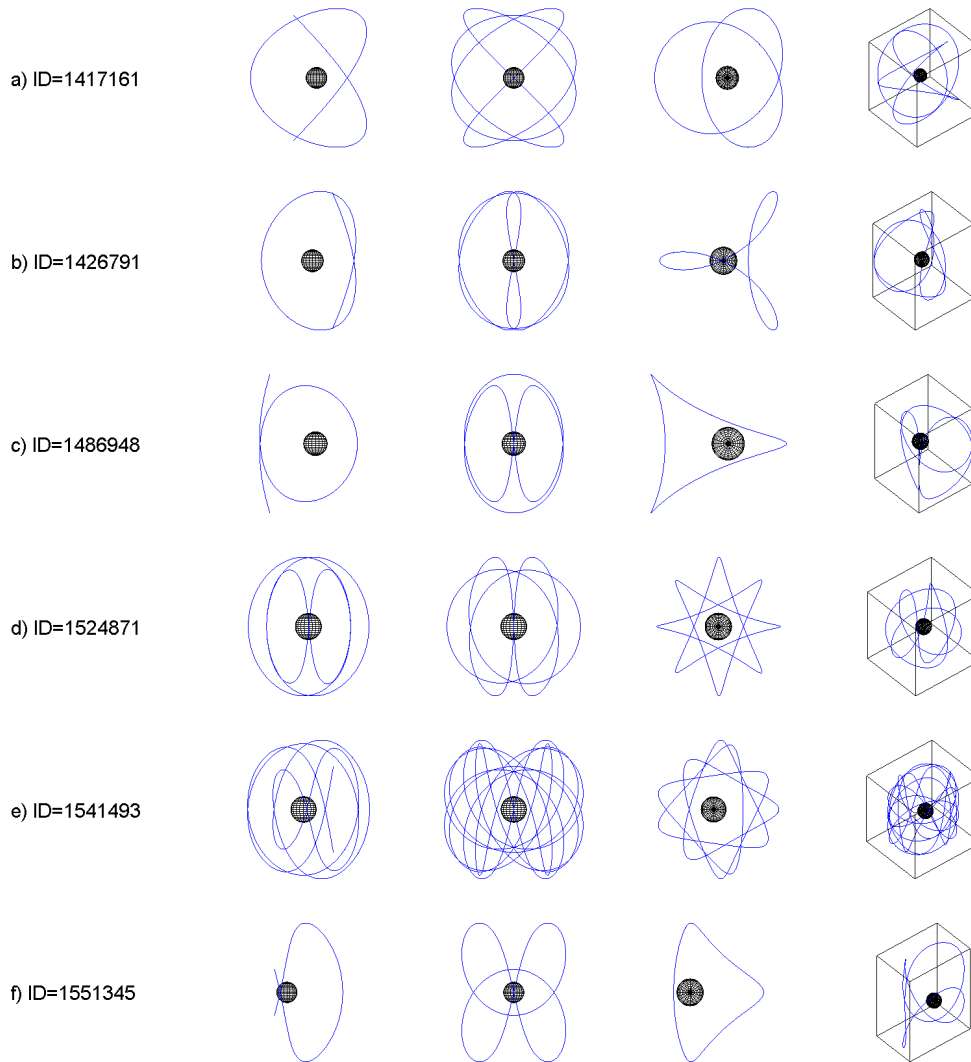


Figure 2: Representative set of unstable periodic orbits around Europa. These orbits act as attracting mechanisms useful for designing capture orbits for mapping missions. Each orbit is illustrated from 4 viewing angles. From left to right: viewed from 1) negative y axis, 2) positive x -axis, 3) positive z axis, 4) azimuth= -130° , elevation= 40° .

Table 4: Initial conditions and characteristics of orbits illustrated in Figure 2^a

<i>ID</i>	#xz plane crossings	x_0 (km)	v_0 (km/s)	w_0 (km/s)	T (days)	J (AU ² /TU ²)	inc. ^b (deg)	min altitude (km)	ratio of min:max altitude	ρ ^c
1417161	8	-9872.93624	0.56390318	0.53604013	4.10426372	3.00079	43.5	8312	0.78	65.06
1426791	8	-7266.22483	0.15356112	0.76160114	3.45364150	3.00173	78.6	5706	0.67	36.69
1486948	4	5544.95918	0.10589302	0.85387058	3.07597199	3.00230	82.9	3984	0.43	126.07
1524871	6	7240.72449	0.03137750	0.69425009	3.41027619	3.00237	87.4	5319	0.76	13.50
1541493	16	8069.76531	0.13751733	0.60543800	9.90252597	3.00249	77.2	3874	0.49	85.60
1551345	4	8547.09184	0.14836010	0.63273862	3.14369851	3.00211	76.8	2406	0.23	10.71

^a Any parameter expressed in un-normalized units is obtained using the length and velocity transformations given in Table 1. Note $y_0 = z_0 = u_0 = 0$.

^b characteristic inclination, range is between 0 and 90°, equal to $\tan^{-1}(w_0 / v_0)$.

^c ρ is a scalar metric of instability. Larger values indicate increasing instability. For linear stability, $\rho=1$.

2. Calculate the Stable Manifolds in RTBP

Once a specific attracting periodic orbit is selected, the stable manifolds are calculated using the stable eigen-directions of the Monodromy matrix as discussed in an earlier section. In Equation (13), a time-like variable, τ , is introduced that varies from 0 \rightarrow 1 and parameterizes the periodic orbit across one full period, where t_τ is the time associated with a specific τ , T is the period, and t_0 corresponds to a reference state on the periodic orbit.

$$t_\tau = t_0 + \tau T \quad (13)$$

The Monodromy matrix, $\Phi(T, t_0)$, is integrated once for the reference state, $\mathbf{X}(t_0)$, and its eigenvalues, λ_i , and eigenvectors, ξ_i , are calculated. Two of eigenvalues are unity. Because the remaining four exist as two sets of reciprocal pairs, two of the eigenvalues will have magnitudes less than unity indicating stability. To proceed, we choose one of the stable eigenvalues.

The eigenvector associated with the chosen stable eigenvalue is the six-vector direction associated with one of the stable manifolds of the periodic orbit. This six-vector can be mapped to a different location along the orbit using the state transition matrix as shown in Equation (14).

$$\xi_\tau = \Phi(t_\tau, t_0)\xi \quad (14)$$

The trajectory on the stable manifold that approaches the periodic orbit at a given τ is approximated by integrating backwards in time the conditions given in Equation (15), where ε is a normalized scalar that perturbs the state in the direction of the stable eigenvector.

$$\mathbf{X}' = \mathbf{X}(\tau) + \varepsilon \|\mathbf{X}(\tau)\| \Re(\xi_\tau) / \|\Re(\xi_\tau)\| \quad (15)$$

The approximated stable manifold then is the set of all trajectories integrated backwards from Equation (15) for $\tau = 0 \rightarrow 1$. As mentioned in an earlier section, the stable manifold from a halo orbit maintains its tube-like structure at great distances and times from its parent orbit. In such cases, the detailed selection of the perturbing ε values has little effect on the structure of resulting manifold. However, in the case of high resonant periodic orbits of interest to this study, the manifolds are not well behaved in general and the selection of the perturbation size can have a significant effect on the behavior and structure of the attracting trajectories.

Table 5 gives a summary of the four parameters available for a mission designer to adjust when generating the attracting trajectories to a specific periodic orbit in the RTBP. Although unnecessary for capture applications, the generation of the unstable manifolds uses the unstable eigenvectors and integrates forward in time, but otherwise follows an identical procedure.

Table 5: Parameters for generating a stable manifold in the RTBP

Parameter	Comment
λ_1 or λ_2	Must choose one of the two stable eigenvalues to obtain the eigenvector for manifold calculation.
ε	The scalar perturbing multiplier for eigen-direction. Can be positive or negative
τ	The time-like variable that parameterizes the periodic orbit. Can take any value from $0 \rightarrow 1$. Choosing the whole range of τ for a given λ and ε allows for the generation of the full manifold.

Figure 3-Figure 8 illustrate a set of attracting trajectories for each of the periodic orbits from Figure 2 for ten equally spaced τ values. Because of xz -plane symmetry, the τ values only vary from $0 \rightarrow \frac{1}{2}$. The associated stable eigenvalue is displayed along with the chosen value of ε .

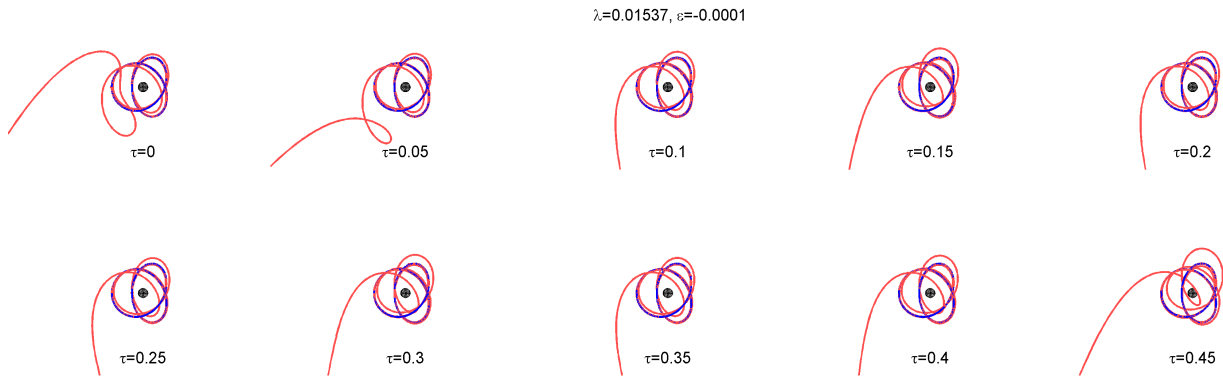


Figure 3: Top view of RTBP capture trajectories to periodic orbit in Figure 2a

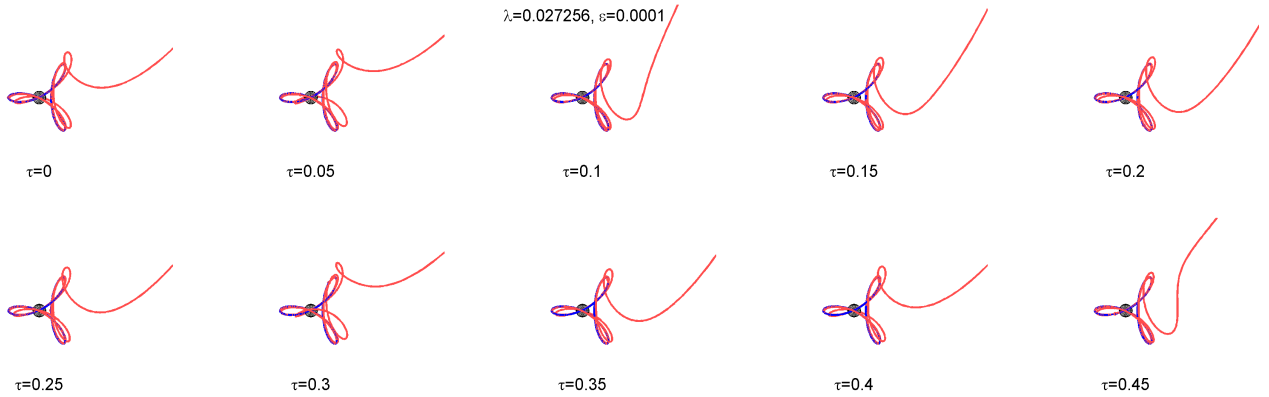


Figure 4: Top view of RTBP capture trajectories to periodic orbit in Figure 2b

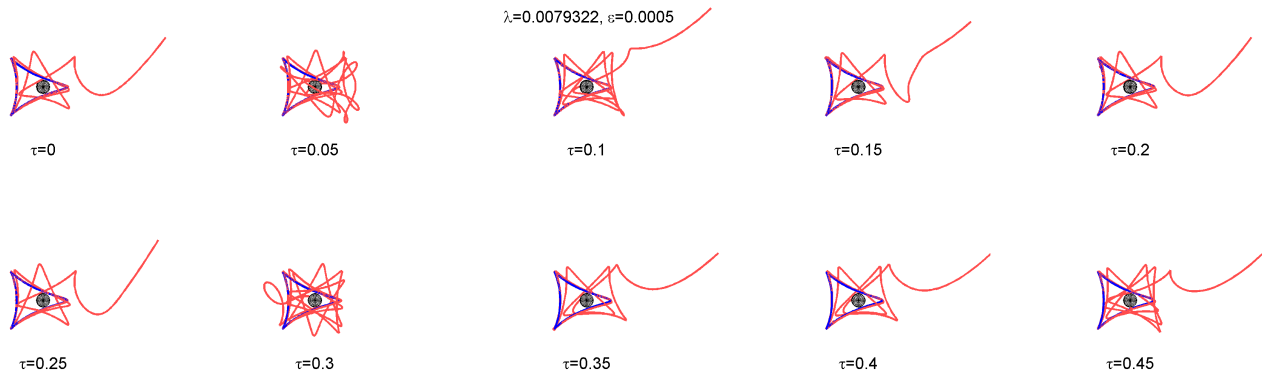


Figure 5: Top view of RTBP capture trajectories to periodic orbit in Figure 2c

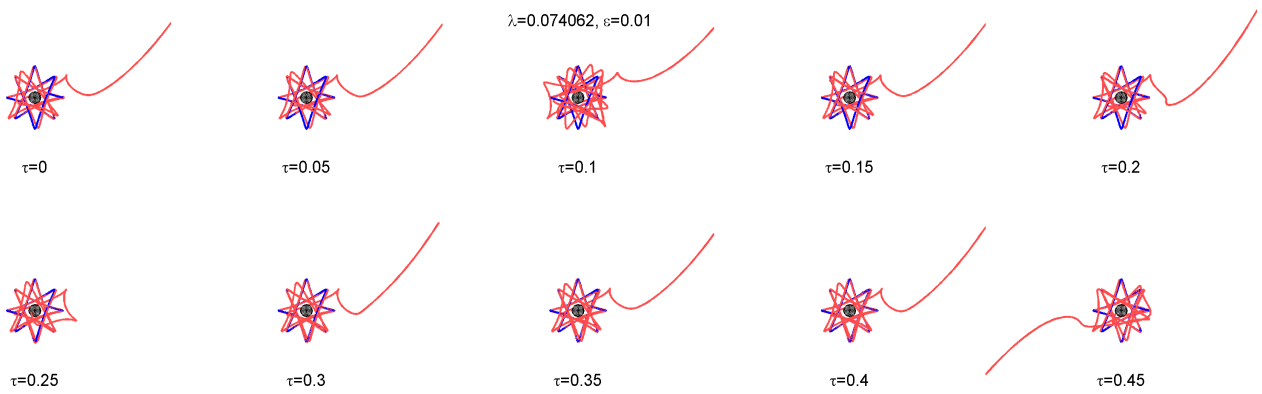


Figure 6: Top view of RTBP capture trajectories to periodic orbit in Figure 2d

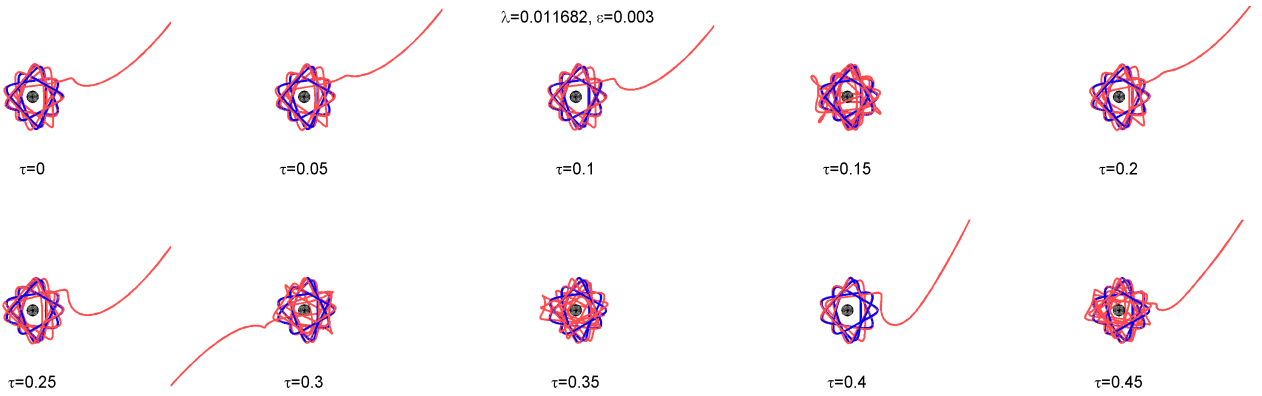


Figure 7: Top view of RTBP capture trajectories to periodic orbit in Figure 2e

$$\lambda = -0.088641 + 0.029464i, \varepsilon = 0.01$$

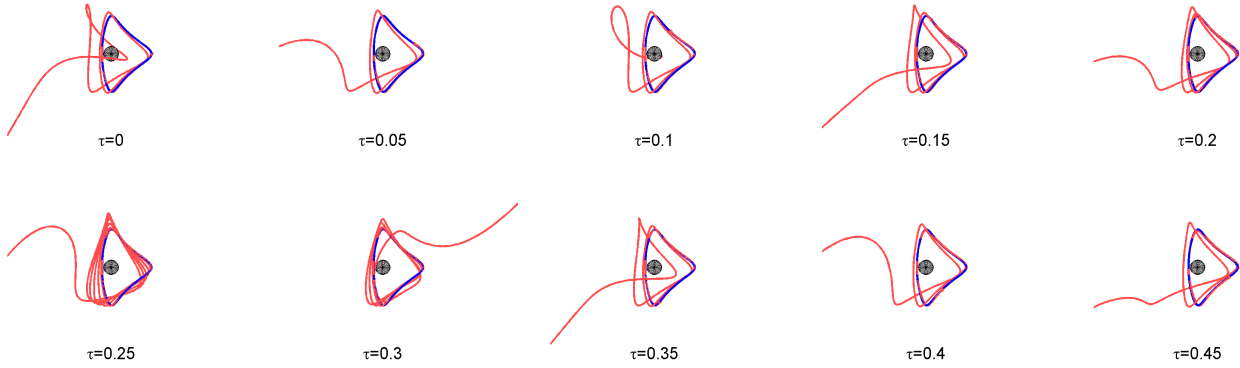


Figure 8: Top view of RTBP capture trajectories to periodic orbit in Figure 2f

The example manifolds in Figure 3-Figure 8 are calculated using the smallest and therefore the most stable eigenvalue for each of the example orbits. In general, the value of ε is selected to be sufficiently small such that the linear region associated with the state transition matrix is not violated, but sufficiently large such that the trajectory departs (in backwards time) the vicinity of the periodic orbit in a reasonable time [14,16]. The radius of the linear region where the state transition matrix well approximates the dynamics scales indirectly with $t-t_0$ (and directly with the magnitude of the eigenvector). Thus, for periodic orbits that close after several revolutions such as those seen in Figure 2, the valid linear region for the state transition matrix over a whole period can be extremely small. It is more important, therefore, to maintain the linear validity for one or two revs rather than the full period. Note that ε can be a negative value because the eigenvector is simply a direction and does not favor forward or backwards. In some cases the positive or negative sign can switch the general capture direction from L2 to L1 or vice versa as demonstrated in Figure 9 (in contrast to Figure 5). Noting that Figure 3 - Figure 9 show just the views from above, Figure 10 illustrates the three-dimensional properties of the example trajectory corresponding to $\tau=0$ from Figure 4.

$$\lambda = 0.0079322, \varepsilon = -1e-006$$

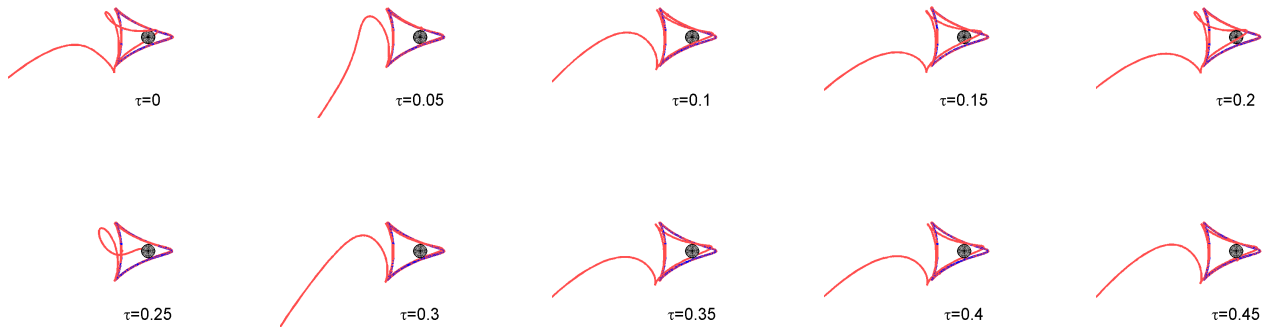


Figure 9: Top view of RTBP capture trajectories to periodic orbit in Figure 2c. Same as Figure 5 except negative ε .

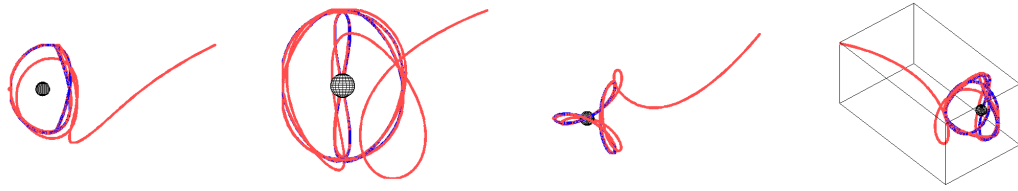


Figure 10: 3D views of attracting trajectory from Figure 4 ($\tau=0$). From left to right: viewed from 1) negative y axis, 2) positive x -axis, 3) positive z axis, 4) azimuth= -130° , elevation= 40° .

The attracting trajectories to the unstable periodic orbits reveal a diverse set of characteristics that can generally be separated into three categories: trajectories that 1) capture from the left through L1, 2) capture from the right through L2, and 3) capture via a path that impacts the surface. While the third category is useful for surface to periodic orbit applications, we are primarily interested in orbits that approach Europa from beyond its sphere of influence. The structure of the attracting trajectories is generally sensitive to the selection of ε , where the degree of sensitivity is highly dependent on the attracting periodic orbit. A value of 0.0001 is generally a good value to try initially; this corresponds to roughly a 1 km perturbation in position and 1 m/s perturbation in velocity. For the examples shown, we varied this guess by several orders of magnitude and selected a value that led to a generally well-behaved manifold. For a given periodic orbit, it is often possible to manipulate the capture orbit to enter near either L1 or L2 through the selection of τ and ε , however, as evidenced by most of the examples, each stable manifold naturally leans towards one direction over the other. Spacecraft coming from Io require captures that pass near L1 (from the left), while spacecraft coming from Callisto or Ganymede require captures that pass near L2 (from the right).

3. Transition to the Ephemeris Model

Once an attracting RTBP periodic orbit and one of its stable manifolds is estimated, we proceed to find analogous capture trajectories in a realistic ephemeris model. Based on the discussion from an earlier section, we take the approach that sacrifices the preservation of the orbit shape for the guarantee of ballistic continuity.

We start by assuming that a given trajectory approaches Europa with appropriate energy levels such that a ballistic capture is feasible (see Figure 11). Obtaining such a trajectory will be discussed briefly in the application section to follow. From the ephemeris approach trajectory, a target seven-state is chosen at a comfortable distance from Europa somewhere in the vicinity of the generated stable manifold. A variety of free parameters in the ephemeris version of the capture trajectory will be selected in order to minimize the miss distance of the backward propagated capture trajectory with the target time, position, and velocity on the approach trajectory. Once an ephemeris capture trajectory is found such that the miss distance is reasonably small, the roles of the target and chaser are reversed and the approach trajectory can then be re-optimized with traditional means to target the seven-state on the ballistic capture trajectory.

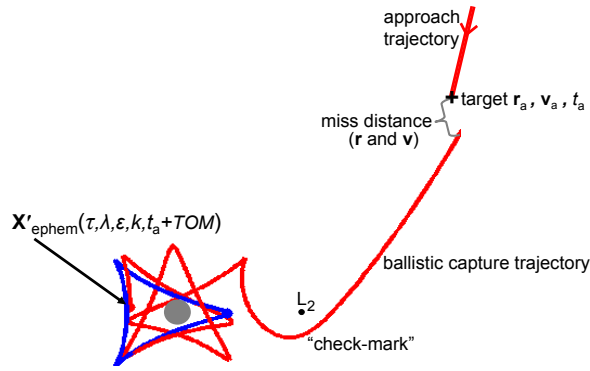


Figure 11: Capture diagram

The several parameters required for mapping a RTBP capture orbit to the ephemeris model are summarized in Table 6. For a given target orbit, τ , ε , and a selection of λ_1 or λ_2 , we have a departing (in reverse time) six-state on the periodic orbit in the RTBP given by Equation (15). This perturbed six vector is mapped to the ephemeris using k and Equations (10)-(12), and is applied at the epoch determined by the target epoch plus the free parameter, TOM , or time spent on the manifold. The resulting perturbed state in the ephemeris, $\mathbf{X}'_{\text{ephem}}$, is a function of all the parameters in Table 6.

Table 6: Free parameters for the ephemeris model mapping

<i>Parameter</i>	<i>Comment</i>
λ_1 or λ_2	The eigenvectors in the RTBP are based on the selection of one of the stable eigenvalues
ε	The scalar perturbing multiplier for eigen-direction. Can be positive or negative.
τ	The time-like variable that parameterizes the periodic orbit. Can take any value from $0 \rightarrow 1$.
k	The scaling parameter that affects the mapping from the RTPB to the ephemeris and accounts for small variations in the Europa-Jupiter distance.
TOM	Time On the Manifold. The epoch is one of the targets on the seven-state on the approaching orbit. Thus, the epoch for departing (in reverse time) the periodic orbit is equal to the target epoch plus TOM . Because the ephemeris model is dependent on the epoch (as opposed to the RTBP) and the epoch of the target state remains fixed, the structure of the capture orbit is significantly changed each time TOM is changed. It is therefore an iterative procedure to patch the ballistic capture trajectory with the approach trajectory.

Generally, we find suitable capture trajectories by guessing reasonable values for all of the parameters except the k scaling parameter, where we automating a one dimensional search to minimize the miss distances in both position and velocity as indicated in Figure 11. Values for τ and the eigenvalue are typically chosen based on the RTBP manifolds and ε and TOM are iterated manually. For the selection of ε , we are no longer concerned with maintaining the linear assumptions of the state transition matrix as we were in the RTBP because we have already sacrificed the preservation of the parent orbit shape. We are primarily concerned only that we find a backward propagated trajectory that leads to a ballistic capture originating in the state space vicinity of the approaching orbit. Thus, we find ε values of $0 \rightarrow 0.05$ to be reasonable guesses. The forward propagation ideally should remain in the vicinity of Europa for several revolutions, but generally the uncontrolled orbit lifetimes are short due to the dominating unstable dynamics.

Figure 12 gives an overview of the algorithm from the selection of the attracting periodic orbit to the final ephemeris target state that ensures a ballistic capture with the desired characteristics. The next section demonstrates the algorithm with a low-thrust transfer from Ganymede to Europa ending in a highly-inclined near circular orbit about Europa.

- 1) Select an unstable RTBP periodic orbit based on desired capture qualities
- 2) Propagate the orbit and variational equations for a full period. Record $\mathbf{X}(\tau)$ for $\tau = 0 \rightarrow 1$ and calculate the eigenvectors and eigenvalues of the Monodromy matrix.
- 3) Using the state transition matrix, map and record each of the two stable two stable eigenvectors, $\xi_i(\tau)$ for $\tau = 0 \rightarrow 1$.
- 4) Approximate the stable manifold in RTBP
 - Select λ_i or λ_2
 - Select ε
 - FOR $\tau = 0 \rightarrow 1$
 - 1) Perturb the $\mathbf{X}(\tau)$ state using $\lambda_i, \xi_i(\tau), \varepsilon$ and Eq. (15)
 - 2) Propagate the perturbed state in reverse time
 - 3) Plot attracting trajectory
 - END τ loop
- 5) Repeat Step (4) until satisfied with manifold characteristics. Note the τ values that lead to *well-behaved* captures in RTBP
- 6) Select an t_a, \mathbf{r}_{a_s} , and \mathbf{v}_a (epoch, position, and velocity) on an ephemeris trajectory that approaches Europa with appropriate energy and geometry
- 7) Search for ephemeris captures that minimize the miss distance to originating state.
 - Select λ_i or λ_2
 - Select ε
 - Select τ
 - Select TOM
 - FOR $k = k_{\min} \rightarrow k_{\max}$ (typically $0.97 \rightarrow 1.03$)
 - 1) Perturb the normalized RTBP $\mathbf{X}(\tau)$ state using $\lambda_i, \xi_i(\tau), \varepsilon$, and Eq. (15)
 - 2) Un-normalize the perturbed state \mathbf{X}' using k, LU^*, TU^* , and Eq. (10)
 - 3) Map the dimensioned perturbed state to the ephemeris using the epoch, $t_a + TOM$, and the mapping described by Eqs. (11) and (12).
 - 4) Propagate the new ephemeris state in reverse time from $t = t_a + TOM$ to $t = t_a$, where the end state is $\mathbf{r}(t_a), \mathbf{v}(t_a)$
 - 5) Calculate and store $\|\mathbf{r} - \mathbf{r}_a\|$ and $\|\mathbf{v} - \mathbf{v}_a\|$
 - END k loop
 - Record \mathbf{r}_b and \mathbf{v}_b : the final conditions associated with the best miss distances.
- 8) Repeat Step (7) until satisfied with the ballistic ephemeris capture trajectory
- 9) Re-optimize the approach trajectory to target the \mathbf{r}_b and \mathbf{v}_b at time t_a to a satisfactory tolerance (~ 10 km, 0.1 m/s)
- 10) Store the converged state as \mathbf{r}_c and \mathbf{v}_c
- 11) Propagate the converged state to a ballistic capture
- 12) After a few revs around Europa, employ low-thrust to stabilize the trajectory and commence a spiral down to the science orbit

Figure 12: Ballistic ephemeris model capture algorithm

APPLICATION: LOW-THRUST GANYMEDE TO EUROPA TRANSFER

We apply the algorithm from Figure 12 to search for a seven-state that will lead to a well-behaved ephemeris capture at Europa. The target periodic orbit, ID=1486948, is chosen and illustrated in Figure 2(c). This orbit has mean two-body eccentricity, inclination, and semi-major axis near 0.2, 65 deg, and 8500 km respectively. Its instability due to the high inclination makes it a difficult target for traditional optimization or targeting tools. Steps (1)-(5) of the algorithm are performed and result in plots similar to Figure 5. For $\lambda = \lambda_1$ (0.027256), it is clear that several values of τ and ε lead to well behaved trajectories that capture through L2. We proceed with step (6) and the design of the ephemeris approach trajectory.

In this example, the approach trajectory is a low-thrust transfer that originates on an escape path from Ganymede. In order to take advantage of the manifold design philosophy using limited control, the approach trajectory must be designed with careful energy and geometry considerations. In general, if the approach trajectory is on or near the *intermoon superhighway*, or the dominating stable manifold associated with the Halo family, it is relatively easy to make minor control adjustments to target the specific capture trajectory of interest. However, with limited control it often not feasible to target a specific close capture trajectory if starting on an approach with energy and geometry appropriate for an entirely different class of orbits, such as a typical DRO type capture [8].

In order to ballistically capture at Europa, it is a necessary (but not sufficient) condition to have the same Jacobi energy as the target periodic orbit. To achieve the Jacobi energies representative of the orbits in Figure 2, thrusting is typically required. However, for limited fuel missions, it is often possible to combine minor thrusting with a string of successive flybys of various bodies to manipulate the geometry, phasing, and energy levels to suit specific mission needs. The leveraging from the flybys is of course controlled by the minimum altitudes, where the smaller altitudes yield larger control. However, thrusting in between flybys is generally required because of a defining characteristic of all of the capture trajectories in Figure 3 - Figure 9.

Note the *check-mark* shape that is upside down when approaching from the left (Figure 9, $\tau=0$) and right side up when approaching from the right (Figure 11 and Figure 5, $\tau=0$). This *check-mark* represents the initial stages of a standard patched conic flyby (expressed in a rotating frame), but the gravity well of Europa proves to be too strong and captures the spacecraft halfway through the flyby. The subtle but important design challenge lies in the placement of the approaching *check-mark*. In all cases in Figure 3 - Figure 9 the approaching *check-mark* finds its extremum near either L1 or L2, and thus the minimum altitude on this approaching flyby is necessarily on the same order as the L1 or L2 distance. In order to maximize the effects of the preliminary Europa flybys, close low-altitude flybys are necessary; however, this is directly opposed to the high-altitude flyby that the final approach is required to mimic in order to be captured. For successive flyby encounters with the same body, thrusting is required to significantly raise or lower minimum altitudes from one flyby to the next. Therefore, a balance of thrusting and *resonant hopping* via successive flybys is typically required to set up a low-energy capture of Europa or any planetary moon. For more detail see References [6] and [7].

The initial guess for the approach trajectory in the present example is shown on the top row of Figure 14. The trajectory consists of 1 Ganymede flyby and 3 Europa flybys prior to the final approach. The two-body energy with respect to Jupiter and the Jacobi constant with respect to Europa histories are illustrated. The flybys and intermediate thrusting are used to target appropriate energy and geometry for a ballistic capture. Note, in the unthrusting case these energy values are only approximately constant in the full ephemeris model. Going back to step (6) from the algorithm, the state \mathbf{r}_a , \mathbf{v}_a , and t_a is selected as a target for the optimization of the ephemeris mapping. The optimization in steps (7) and (8) are performed and the best resulting state, \mathbf{r}_b and \mathbf{v}_b , that leads to an ephemeris capture is illustrated in Figure 13. The optimized parameters including the k scaling factor are listed in the caption. Note the resemblance to its corresponding RTBP trajectory in Figure 5 ($\tau=0.2$).

Next, from step (9), the full approach trajectory from Ganymede is retargeted and reoptimized with Mystic using the new target state \mathbf{r}_b and \mathbf{v}_b . The resulting trajectory converges to the final state \mathbf{r}_c and \mathbf{v}_c within 2 km in position and and 4 cm/s in velocity. Although the trajectories are highly sensitive in nature, tolerances of 10 km and 100 m/s are generally sufficient to maintain the desired structure of the capture. The converged approach trajectory and energy history are illustrated in the bottom row of Figure 14. Note, the optimizer primarily adjusts the third Europa flyby and raises perijove with thrusting prior to the final approach.

Table 7: Resulting states for the example ephemeris capture at Europa

<i>Description</i>	<i>Value</i> ^a
The seven-state selected from the ephemeris approach trajectory that is a priori in the vicinity of a feasible capture in terms of geometry and energy. The subscript a represents approach.	$\mathbf{r}_a = (-1.07883310\text{E}+05, 2.87668841\text{E}+04, 1.23441619\text{E}+04)$ km $\mathbf{v}_a = (1.72006636\text{E}+00, -1.81673502\text{E}+00, -3.02506277\text{E}-01)$ km/s $t_a = 2460919.10489252$ Julian Date
The seven-state that results from the optimization of the parameters given in Table 6 for the mapping to ephemeris model. The subscript b represents best.	$\mathbf{r}_b = (-1.01918183\text{E}+05, 3.41628884\text{E}+04, 1.74521592\text{E}+04)$ km $\mathbf{v}_b = (1.65707274\text{E}+00, -1.88920203\text{E}+00, -5.60147066\text{E}-02)$ km/s $t_b = t_a$
The converged state after optimizing the approach trajectory with the new target state (\mathbf{r}_b , \mathbf{v}_b , t_a). The subscript c represents converged.	$\mathbf{r}_c = (-1.01919709\text{E}+05, 3.41616621\text{E}+04, 1.74520496\text{E}+04)$ km $\mathbf{v}_c = (1.65708924\text{E}+00, -1.88923145\text{E}+00, -5.60167814\text{E}-02)$ km/s $t_c = t_a$

^a positions and velocities are relative to Europa in the non-rotating J2000 frame.

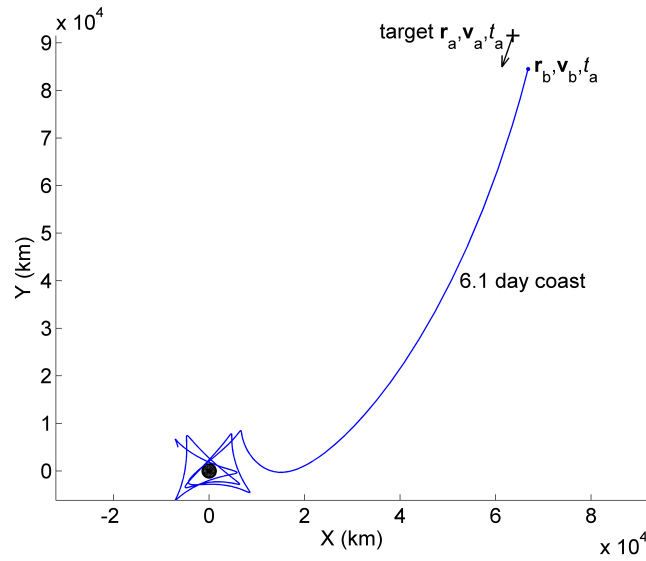


Figure 13: Ephemeris ballistic capture trajectory resulting from algorithm given in Figure 12. Optimized parameters: attracting periodic orbit ID=1486948, $\lambda = \lambda_1$ (0.027256), $\varepsilon = 0.03$, $\tau = 0.2$, TOM=6.1 day, $k = 0.10053947$

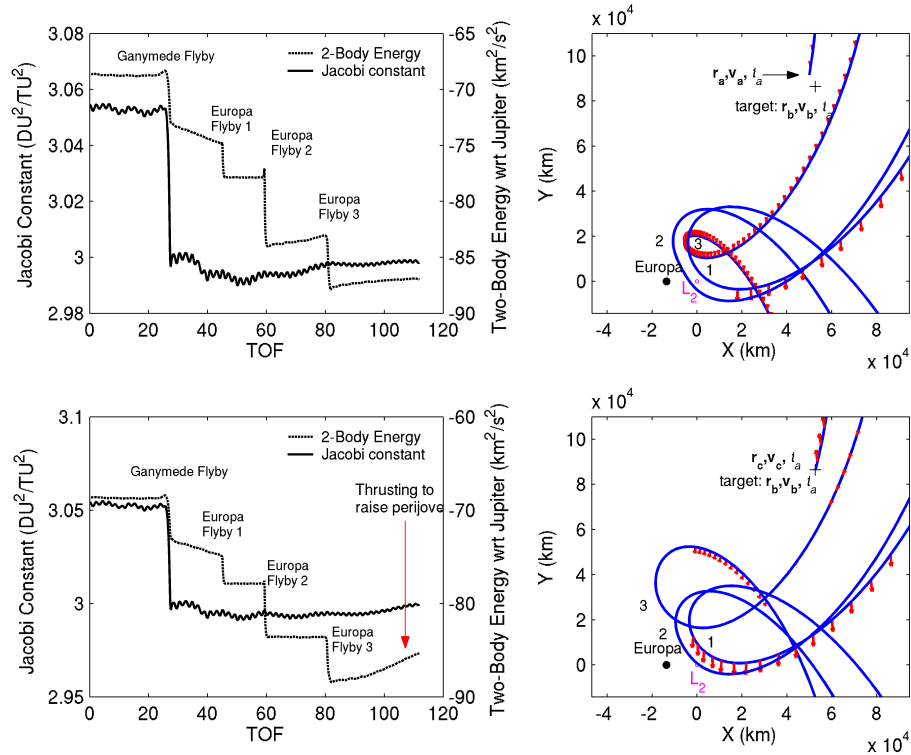


Figure 14: Example low-thrust ephemeris transfer from Ganymede to the vicinity of Europa. Arrows on the trajectory indicate thrusting. Top row: initial guess. Bottom row: converged trajectory that leads to a ballistic capture when propagated further. See Table 7 for relevant states.

Finally, the trajectory design is completed by ballistically propagating the converged approach state to a close highly inclined capture state about Europa. Following a 2.3 day ballistic coast that captures through L2 and completes a full revolution around Europa, low-thrust again is used to maintain the orbit and start to spiral down towards the science orbit. Figure 15 illustrates the final optimized trajectory. The continuation to the science orbit is omitted for clarity although it is straightforward to implement. Note the structure of the capture orbit is remarkably well-behaved despite existing in a highly chaotic and unstable region. While the final capture orbits are clearly dependent on both the epoch and ephemeris, the basic characteristics of the orbits are generally reproducible because the technique is based largely on the time invariant model of the RTBP.

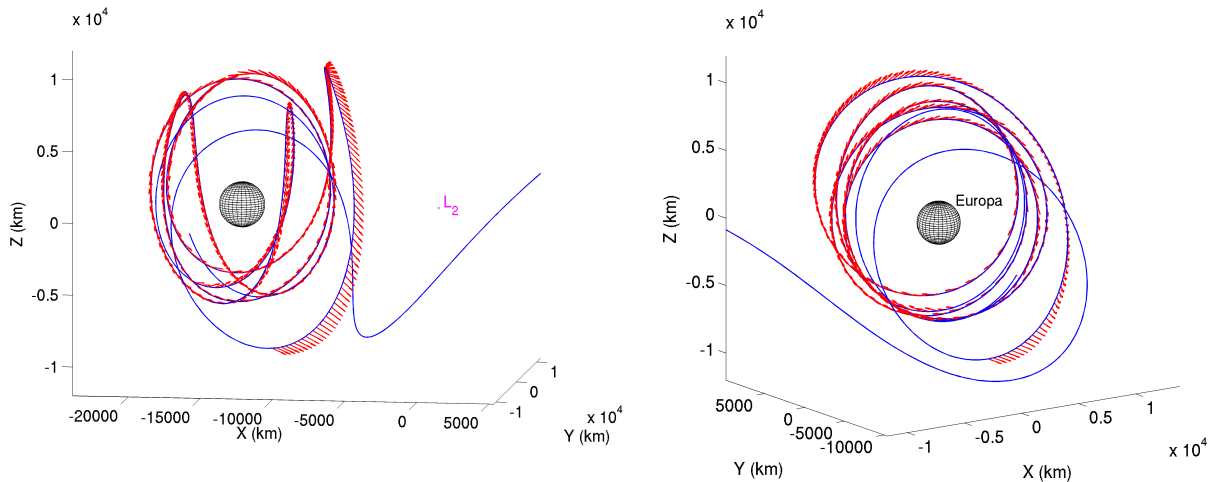


Figure 15: Continuation of the converged trajectory from Figure 14. Ballistic 2.3 day ephemeris capture followed by 4.3 days of optimized low-thrust maneuvers (acceleration $\sim 0.13 \text{ mm/s}^2$) to finish in a near 2 body orbit with eccentricity ~ 0.003 , inclination $\sim 71 \text{ deg}$. and semi-major axis near 7280 km. Left: Rotating frame. Right: Non-rotating frame.

CONCLUSIONS

The main contributions of this paper are as follows: 1) Dynamical systems theory is successfully applied to several unstable periodic orbits that circulate around Europa, and the behavior of the associated stable manifolds are investigated and documented. 2) The subtleties associated with mapping these simple model manifolds into a realistic model are explored and an algorithm is presented to find and target efficient ballistic captures using a full ephemeris. 3) Lastly, the presented technique is systematic and allows a mission designer to target specific characteristics of a capture state using little control authority even in the notably unstable environments such as highly-inclined orbits about Europa. Although close capture trajectories around Europa are the focus of this paper, the technique is applicable for capture or escape from any unstable periodic orbit in any dynamical system.

ACKNOWLEDGEMENTS

The authors acknowledge Jon Sims, Greg Whiffen, Anil Hirani, and Anastassios Petropoulos for contributing discussions and support. Part of this work was carried out at the Jet Propulsion Laboratory, California Institute of Technology, under a contract with the National Aeronautics and Space Administration.

REFERENCES

- [1] Scheeres, D.J., Guman, M.D., Villac, B.F., “Stability Analysis of Planetary Satellite Orbiters: Application to the Europa Orbiter,” *Journal of Guidance, Control, and Dynamics*, Vol. 24, No. 4, 2001, pp. 778–787.
- [2] Lara, M., San-Juan, J.F., “Dynamic Behavior of an Orbiter Around Europa.” *Journal of Guidance, Control and Dynamics*, Vol. 28, No. 2, 2005, pp. 291–297.
- [3] Aiello, J., “Numerical Investigation of Mapping Orbits about Jupiter’s Icy Moons,” paper AAS 2005-377, presented at the Astrodynamics Specialists Conference, Lake Tahoe, California, August 2005.
- [4] Lam, T., Whiffen, G. J., “Exploration of Distant Retrograde Orbits around Europa,” Paper AAS 05-110, presented at the 15th Spaceflight Mechanics Meetings, Copper Mountain, Colorado, January 2005.
- [5] Paskowitz, M. E., Scheeres, D.J., “Transient Behavior of Planetary Satellite Orbiters”, AAS paper 05-358, presented at the 2005 AAS/AIAA Astrodynamics Specialist Conference in Lake Tahoe, California, August 2005.
- [6] Whiffen, G. J., “An investigation of a Jupiter Galilean moon orbiter trajectory”, Paper AAS 03-544. Presented at the AAS/AIAA Astrodynamics Specialist Conference, Big Sky, Montana, August, 2003.
- [7] Whiffen, G. J., “Jupiter Icy Moons Orbiter Reference Trajectory,” Paper AAS 06-186, presented at the AAS/AIAA Space Flight Mechanics Meeting, Tampa, Florida, 2006.
- [8] Lam, T., Hirani, A. N., “Characteristics of Transfers to and Captures at Europa,” Paper AAS 06-188, presented at the AAS/AIAA Space Flight Mechanics Meeting, Tampa, Florida, 2006.
- [9] Koon, W.S., Lo, M. W., Marsden, J.E., Ross S.D., “Low Energy Transfer to the Moon,” *Celestial Mechanics and Dynamical Astronomy*, Vol. 81, No. 1-2, Sept. 2001, pp. 63-73.
- [10] Lo, M.W., Anderson, R.L., Whiffen, G.J., “The Role of Invariant Manifolds in Low Thrust Trajectory Design,” Paper AAS 04-228, AAS/AIAA Spaceflight Dynamics Conference, Maui, Hawaii, February 8-12
- [11] Lo, M. W., Parker, J. S., “Unstable Resonant Orbits near Earth and Their Applications in Planetary Missions,” Paper AAS 04-5304, AIAA/AAS Astrodynamics Specialist Conference and Exhibit, Providence, RI, Aug. 16-19 2004.
- [12] Gómez, G., Koon, W. S., Lo, M. W., Marsden J. E., Masdemont J., Ross S. D., “Connecting orbits and invariant manifolds in the spatial restricted three-body problem,” *Nonlinearity*, Vol. 17, No. 5, September 2004, pp. 1571-1606.
- [13] Gomez, G., Koon, W.S., . Lo, M.W., Marsden, J.E., Masdemont, J., Ross, S.D. , "Invariant Manifolds, The Spatial Three-Body Problem and Space Mission Design," Paper AAS 01-301, AAS/AIAA Astrodynamics Specialist Conference, Quebec City, Canada, Paper AAS 01-301, July 2001.
- [14] Senet, J., Ocampo, C., “Low-Thrust Variable Specific Impulse Transfers and Guidance to Unstable Periodic Orbits,” *Journal of Guidance, Control, and Dynamics*, Vol. 28, No. 2, 2005, pp. 280–290.
- [15] Serban, R., Koon, S.K., Lo, M.W., Marsden, J.E., Petzold, L.R., Ross, S.D., Wilson, R.S., “Halo Orbit Mission Correction Maneuvers Using Optimal Control,” *Automatica*, Vol 38, No. 4, April 2001, pp. 571-583.
- [16] Howell, K.C., Barden,, B.T., Lo, M.W., “Application of Dynamical Systems Theory to Trajectory Design for a Libration Point Mission,” *The Journal of the Astronautical Sciences*, Vol. 45, No. 2, April-June 1997, pp. 161-178.
- [17] Belbruno, E., “A Low Energy Lunar Transportation System Using Chaotic Dynamics”, AAS paper 05-382, presented at the 2005 AAS/AIAA Astrodynamics Specialist Conference in Lake Tahoe, California, August 2005.
- [18] Lo, M. W., “The Lunar L1 Gateway: Portal to the Stars and Beyond,” Paper 2001-4768, Presented at the AIAA Space Conference, Albuquerque, New Mexico, 2001.
- [19] Villac, B., Lara, M., “Stability Maps, Global dynamics, and Transfers”, AAS paper 05-378, presented at the 2005 AAS/AIAA Astrodynamics Specialist Conference in Lake Tahoe, California, August 2005.
- [20] Farquhar, R.W., Muhonen, D.P., Newman, C.R., Heuberger, H.S., “Trajectories and Orbital Maneuvers for the First Libration Point Satellite,” *Journal of Guidance and, Control*, Vol. 3, No. 6, 1980, pp. 549–554.
- [21] Sharer, P., Harrington, T., “Trajectory Optimization for the ACE Halo Orbit Mission”, AAS paper 96-3601, presented at the AAS/AIAA Astrodynamics Conference in San Diego, California, July 1996.

- [22] Roberts, C.E., “The SOHO Mission L1 Halo Orbit Recovery From the Attitude Control Anomalies”, presented at the Libration Point Orbits and Applications Conference, Parador d’Aiguablava, Girona, Spain, 10-14 June 2002.
- [23] Koon, W.S., Lo, M.W., Marsden, J.E., Ross, S.D., “The Genesis Trajectory and Heteroclinic Connections”, AAS paper 99-451, presented at the 2005 AAS/AIAA Astrodynamics Specialist Conference in Girdwood, Alaska, August 1999.
- [24] Howell, K.C., Barden, B.T., Wilson, R.S., Lo, M.W., “Trajectory Design Using a Dynamical Systems Approach with Applications to Genesis,” Paper AAS 97-709, presented at the AAS/AIAA Astrodynamics Specialist Conference, Sun Valley, Idaho, August 1997.
- [25] Russell, R. P., “Global Search for Planar and Three-dimensional Periodic Orbits Near Europa,” Paper AAS 2005-290, presented at the 2005 AAS/AIAA Astrodynamics Specialist Conference, Lake Tahoe, California, August 2005.
- [26] Hirani, A.H., Lo, M.W. “Surface Structure of an Invariant Manifold of a Halo Orbit,” Paper AAS 2005-379, presented at the 2005 AAS/AIAA Astrodynamics Specialist Conference, Lake Tahoe, California, August 2005.
- [27] Lara, M., Russell, R.P., Villac, B., “On Parking Solutions Around Europa”, AAS paper 05-384, presented at the 2005 AAS/AIAA Astrodynamics Specialist Conference in Lake Tahoe, California, August 2005.
- [28] *Jupiter, The Planet, Satellites, and Magnetosphere*, edited by F. Bagenal, T. Dowling, W. McKinnon, Cambridge Planetary Society, Cambridge, United Kingdom, 2004. pp. 36, 347.
- [29] Battin, R. H., *An Introduction to the Mathematics and Methods of Astrodynamics*, American Institute of Aeronautics and Astronautics, Inc., New York, 1987, pg. 453.
- [30] *Applied Nonlinear Dynamics*, Nayfeh, A. H., Balachandran, B., John Wiley and Sons, Inc., New York, 1995. Sec. 3.2.
- [31] *Foundations of Applied Mathematics*, Greenberg, M.D., Prentice-Hall, Inc., Englewood Cliffs, New Jersey, 1978. pg. 333.
- [32] Broucke, R., “Stability of Periodic Orbits in the Elliptic, Restricted Three-Body Problem,” *AIAA Journal*, Vol. 7, No. 6, 1969, pp. 1003-1009.
- [33] Lara, M., Russell, R.P., “On the Design of a Science Orbit about Europa,” Paper AAS 06-168, presented at the AAS/AIAA Space Flight Mechanics Meeting, Tampa, Florida, 2006.
- [34] Standish, E. M., *JPL Planetary and Lunar Ephemerides*, CD-ROM, Willman-Bell Inc., Richmond, VA, 1997.
- [35] Seidelmann, P.K., Abalakin, V.K., Bursa, M., Davies, M.E., Bergh, C. de, Lieske, J.H., Oberst, J., Simon, J.L., Standish, E.M., Stooke, P., Thomas, P.C., “Report of the IAU/IAG Working Group on Cartographic Coordinates and Rotational Elements of the Planets and Satellites: 2000,” *Celestial Mechanics and Dynamical Astronomy*, Vol. 82, Issue 1, 2002, pp. 83–111.
- [36] *Geophysical Geodesy*, Lambeck, K., Clarendon Press, Oxford, 1988. Sec. 2.2.
- [37] Whiffen, G. J., Sims, J. A., “Application of the SDC optimal control algorithm to low-thrust escape and capture trajectory optimization”, Paper AAS 02-208. Presented at the AAS/AIAA Space Flight Mechanics Meeting, San Antonio, Texas, 2002.